JOURNAL OF OPTOELECTRONICS AND ADVANCED MATERIALS Vol. 12, No. 3, March 2010, p. 616 - 620

Direct ablation of ZnO with UV and IR laser for thin film solar modules

S. KU[a,b*], S. HAAS[a], G. SCHOEPE[a], B. E. PIETERS[a], Q. YE[b], U. RAU[a]
[a] *IEF-5-Photovoltaik, Forschungszentrum Jülich, D-52425 Jülich, Germany*
[b] *Department of Physics, Shanghai Jiao Tong University, 200240 Shanghai, China*

A common procedure to pattern transparent conductive oxides (TCO) for monolithic series connection of thin-film solar modules is to use an infrared (IR) laser incident from the glass side. However, for cheaper opaque substrates this standard procedure cannot be applied and the films need to be ablated directly from the film side. In this article we used two Nd-doped solid state pulsed lasers to pattern as-deposited in-house aluminum doped zinc oxide (ZnO:Al) thin-films from the film side. One IR laser with a wavelength of 1064nm (photon energy less than the band-gap of ZnO) and one UV laser with a wavelength of 355nm (photon energy larger than the band-gap of ZnO) were used. For single pulses a smoother ablation of ZnO was obtained with the UV laser compared to the IR laser. Furthermore, using the UV laser we obtained craters with a lower rim and less material melt. The ablation thresholds were determined with three different methods. The ablation threshold of ZnO for the IR is larger than for the UV. The differences in ablation thresholds are explained by the differences in absorption coefficients of the ZnO for the IR and UV. Both wavelengths can achieve good electrical separation even after deposition of a highly conductive µc-Si:H p-layer. In order to compare the various laser processes we prepared 10cm×10cm µc-Si:H modules on ZnO. We obtained comparable results for modules patterned from the film-side and modules patterned with the standard process.

(Received June 22, 2009; accepted January 11, 2010)

Keywords: Laser patterning, Ablation threshold, Electrical separation, Solar modules

1. Introduction

An infrared (IR) laser is commonly used to pattern transparent conductive oxides (TCO) for monolithic series connection of thin-film solar modules. By scribing through the glass, the free carrier absorption starting at the glass-TCO interface leads to a high pressure vapor layer that removes the ZnO [1-2]. However, cheaper opaque substrates require a direct ablation from the film side, where the film is ablated entirely through thermal evaporation [1, 3]. This mechanism is less efficient and a high ridge is often observed around the ablated crater due to melting [4]. A UV laser with a wavelength of 355 nm is considered to be a more suitable laser source for this purpose because of the higher absorption of ZnO at this wavelength compared to the absorption due to free carriers in the IR wavelength range.

In this paper, we compared the ablation properties of UV and IR laser on ZnO films. We first study ablation in single pulse ablation experiments where we compare crater morphologies and the ablation thresholds. We used three methods to determine ablation thresholds, differential, integral and radius method. To investigate the application of laser pattering in the thin-film µc-Si:H solar modules, the electrical separation of laser patterned lines was analyzed. Finally we present µc-Si:H modules to compare the quality of the laser lines obtained with the various scribing processes.

2. Experimental

Two diode-pumped Q-switched laser sources, neodymium-doped lasers with a fundamental wavelength of 1064nm and a third harmonic wavelength of 355nm, were used in this work. Both lasers were adjusted to work in TEM_{00} mode. A laser pulse intensity profile measurement setup (Primes Microspotmonitor) was used to obtain single pulse intensity profiles in the focus range. The full width at half maximum (FWHM) pulse duration was τ_{pulse}=10-20ns for both lasers. A worktable with a split-axis-system allows positioning in the substrate plane with a resolution of 1µm and a linear Z-axis allows focusing the beam on the film surface.

All samples used in this work were corning glass covered with in-house ZnO which were sputtered from a $ZnO:Al_2O_3$ (99:1wt%) target at a substrate temperature of 300°C and 0.1Pa pure argon atmosphere. The thickness of as-deposited ZnO was around 800nm. More details on the ZnO properties and deposition conditions can be found elsewhere [5]. Scanning Electron Microscopy (SEM) images were taken of craters after laser ablation to evaluate the ablation surface morphology. Scanning Confocal Microscopy (SCM) was used to obtain 3D depth-profiles of the laser ablated craters. A Keithley Source Meter was used to measure resistance of laser patterned lines.

3. Results and discussion

3.1 Determination of ablation threshold

Single pulse laser ablated craters are compared to the laser pulse profiles. The photon energy of the IR light (1.17eV) is lower than the band gap of ZnO (3.4eV). Thus free carrier absorption of IR photons causes heating and subsequent melting and evaporation of the ZnO. From Fig. 1(a) it can be seen that molten material was ejected out of the crater and there are cracks at the crater surface, presumably due to thermal stress. The motion of molten material also causes an irregular depth profile of the IR ablated crater and a rim of more than 300nm high at the edge of the crater, see Fig. 1(b). The SEM image of UV ablated crater Fig. 1(c) shows much less molten material during ablation. This can be explained by the higher absorption and shorter penetration depth of UV laser, causing more heat in smaller volume of material than for the IR laser. The crater profile in Fig. 1(d) shows a smoother profile and a much lower rim of around 30nm high.

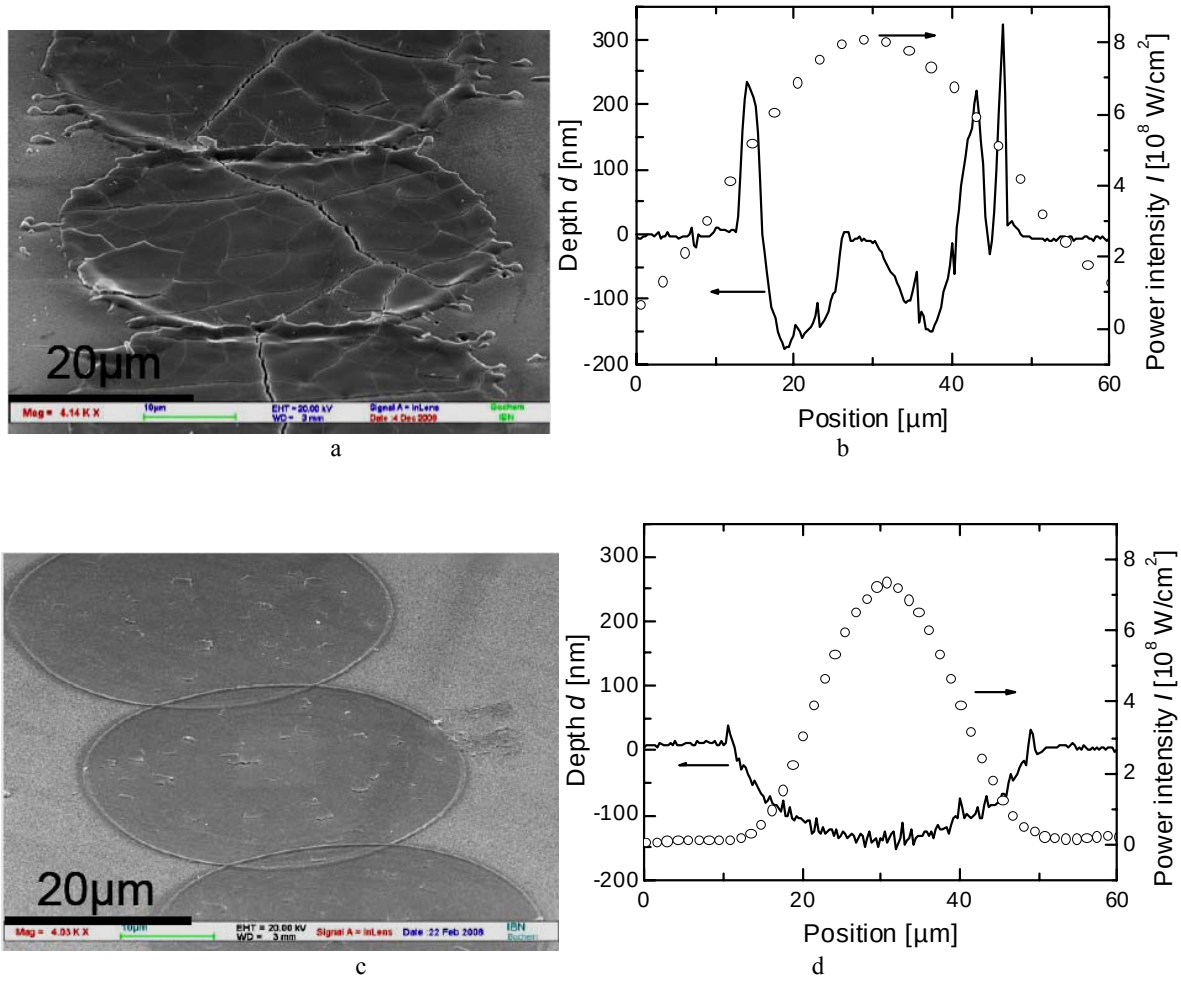

Fig. 1. (a) The SEM image of single pulse IR laser ablated crater and (b) its corresponding cross-section intensity profile and ablated crater. (c) The SEM image of single pulse UV laser ablated crater and (d) its corresponding cross-section intensity profile and ablated crater. IR with single pulse energy 150.6µJ, UV with single pulse energy 31µJ.

In order to compare ablation thresholds of the UV and IR, we scaled the laser intensities by the absorptance which was computed from low intensity reflection-transmission measurements on the ZnO substrates (1-*R*-*T*). We first determined the ablation threshold from a single pulse ablation experiment. We directly use the intensity and its corresponding ablation depth at a single position in the crater (see Fig. 1 (b) for IR and (d) for UV). With this differential method we can thus obtain the ablation depth versus intensity with laser intensities up to the peak of Gaussian beam. The relation between the ablation-depth and laser intensity becomes approximately linear in a semi-logarithmic plot. The ablation depth as a function of intensity can be described by [7]

$$d(I)=A\ \ln(I/I_{th}), \qquad (1)$$

where d is the ablation-depth, A is a constant, and I_{th} is the ablation threshold. By fitting Eq. (1) to single pulse experiment data we obtained the differential ablation thresholds (see Fig.2). The differential ablation threshold for the UV laser is 9.4×10^6 W/cm^2 . For IR laser (Fig.2(b)), there is significant lateral movement of molten material during ablation. Therefore, the crater profile does not correspond to the laser intensity and the differential method does not exhibit a monotonically increasing ablation-depth as a function of intensity. Furthermore, the ablation depth is sometimes negative due to the formation of the high rim around the crater which is possibly due to voids. For these reasons the differential method does not produce a meaningful ablation threshold for the IR laser.

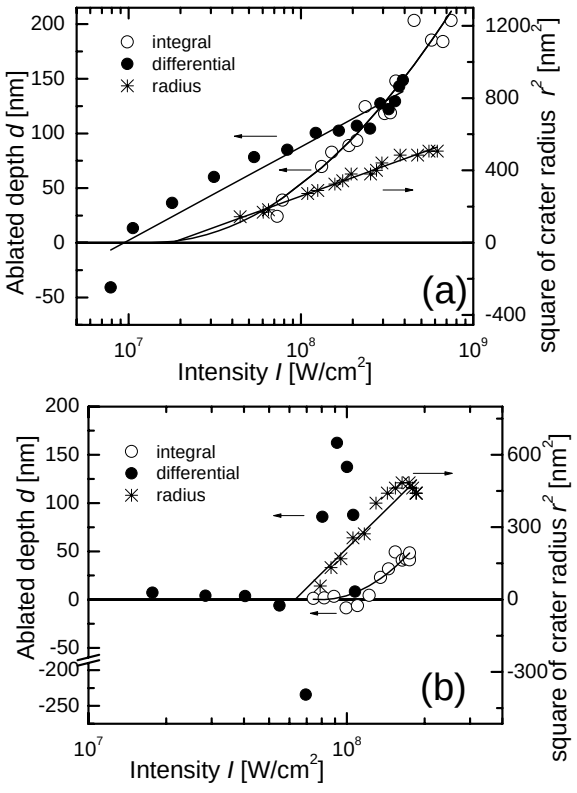

Fig.2. The ablation-depth (left y axis) and square of laser ablated pulse crater radius (right y axis) as a function of laser intensity. Open circles: Integral method. Filled circles: Differential method. Stars: square of radius. The intensities are corrected for the absorptance. The solid lines are the fittings of the data. (a) UV laser. (b) IR laser, note that the ablation-depth axis has a break from -60 to -190. The differential methods data is from Fig.1(b), (d).

In the integral method we want to eliminate the influence of heat diffusion and lateral movement of material. It is expected that heat diffusion leads to a larger diameter of the crater at the expense of a reduced maximum depth of the crater. We now assume that these two effects compensate for each other, leading to the same ablated volume as when there was no heat and lateral movement of material. We ablated craters with different laser intensities and computed the volume of these craters from the 3D SCM measurements. In order to compare with the differential method, the average ablated depth of the crater, d_{avr}, was computed by dividing the volume by the pulse size calculated using the $1/e^2$ criterion on the laser intensity profile. An expression for the ablated volume was obtained by integrating Eq. (1) over the Gaussian intensity profile. The resulting expression for the average ablated depth versus intensity is $d_{avr}(I)=A\ \ln^2(I/I_{th})$. By fitting this expression to the data we obtained integral ablation threshold, 1.34×10^7 W/cm^2 and 7.9×10^7 W/cm^2 for UV and IR respectively. The integral method also shows a non-monotonic increase of the ablation-depth versus intensity for IR. It can be seen that upon increasing laser power the ablation-depth first becomes negative which indicate the material becomes less dense, possibly due to voids. However the non monotonous ablation versus intensity for the integral method is much less severe than for the differential method, allowing to determine the threshold for the IR laser.

As a third method we used the method described in reference [6]. The relation between the laser intensity and the radius of the crater ablated with a Gaussian beam follows $r^2=\rho^2 \ln(I/I_{th})$ where r is the crater radius, ρ is the spatial radius of laser beam using the 1/e criterion on the laser intensity profile. The ablation thresholds according to this radius method are 1.8×10^7 W/cm^2 and 6.3×10^7 W/cm^2 for UV and IR which are close to the ablation thresholds obtained with the integral method.

From the threshold determined for the UV laser with the various methods it can be seen that the differential method gives the lowest estimate to the threshold. This can be explained with heat diffusion, leading to a larger diameter of the crater.

The ablation thresholds for the IR laser are higher than the ablation thresholds for the UV laser (a factor 3.5 and 5.9 according to the radius and integral method, respectively). From Fig.1(a) it can be seen that with the IR laser molten material was re-solidified. The SEM image of the UV process shows no sign of molten material. This suggests that, compared to the UV process, in the IR process there is more energy lost to heating and melting material which is not ablated in the process. This energy loss may be the cause for more thermal stress in the ZnO, which could explain why the cracking observed in Fig.1(a) is only observed for the IR process. These results support the thesis that the higher absorption coefficient of ZnO for the UV laser leads to a more efficient ablation process.

3. 2. Determination of electrical separation and application in solar modules

To electrically separate adjacent parts of the ZnO film, the laser pulse repetition frequency and the table speed were adjusted to pattern continuous lines. As-deposited 10cm×10cm ZnO substrates were used. The total length of the patterned each laser line was 80mm. UV laser lines have lumps at the edges of the lines, which are probably caused by re-deposition of ablated ZnO. For the IR laser, there is a large rim and flakes around the lines due to

molten material ejection. We followed the standard procedure to manufacture µc-Si:H solar cells, where after the scribing of the ZnO, the ZnO is texture etched for 30 seconds in HCl. The texture-etch serves to enhance light trapping in the solar modules. After etching the ZnO had a thickness of around 650nm and the accumulated material at the edges of the laser lines was completely removed for both laser processes. The resistance over each line is larger than 60MΩ after etching for all lines.

In the thin-film silicon solar module production process a highly conductive µc-Si:H p-layer is deposited on the laser patterned ZnO substrates. This µc-Si:H p-layer constitutes a shunt resistance over the cell stripes as it connects two adjacent ZnO stripes. We therefore studied the separation property of laser lines after the deposition of a typical µc-Si:H p-layer. We separated the lines into several sections, each 10mm in length (l), by standard laser patterning from glass-side with the IR laser. A Keithley Source Meter was used to measure the resistance of these lines (R) directly at room temperature. As the lateral conductivity of the TCO layer is much higher than the thin µc-Si:H p-layer, the resistance is dominated by the p layer in the laser scribed lines. The measured value for the resistances were used to calculate the "electrical width" of the lines which is defined as w=R l/ $R_{\square}$ where $R_{\square}$ is the sheet resistance of p layer. The visual width was the width of laser lines measured using an optical microscopy image. In Fig.3 we show the electrical width as a function of the visual width. It can be seen that for all laser parameters the electrical width is smaller than the visual width, indicating there may be residual ZnO in the lines. Using both lasers from film side (filled symbols in Fig.3) we can obtain laser lines with a comparable electrical width to the standard process (open symbols in Fig.3). As laser lines constitute dead area in solar module, we want to obtain a good electrical separation between adjacent stripes at a minimal line width. Fig.3 shows that we can achieve good electrical separation (comparable with the standard process) with thin lines scribed from the film side

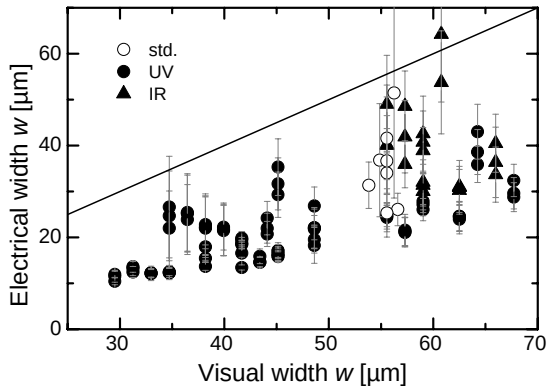

Fig.3. Electrical width versus visual width for 10mm-length laser lines covered with a µc-Si:H p-layer. Std.: laser lines patterned with standard procedure (IR laser from glass side). The straight line indicates where electrical width equals to visual width.

In order to compare the various laser processes we prepared 10cm×10cm µc-Si:H p-i-n modules on ZnO under standard deposition conditions [8]. One reference module was prepared using the standard TCO patterning process. The other two modules were prepared using TCO patterning with the UV or the IR from the film side. For all modules the active layers and back contact layers were patterned using the standard process. Fig.4 shows the IV curve of the 3 modules under AM1.5 illumination. With all TCO patterning processes we obtained comparable results.

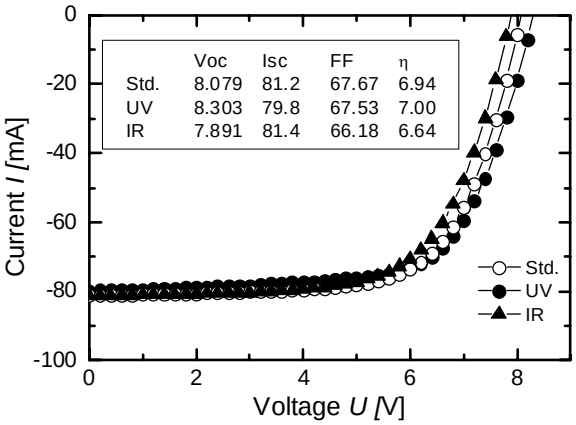

Fig. 4. Current-Voltage curves of 10cm×10cm µc-Si:H modules measured under AM1.5 spectrum. For two samples (UV and IR) the ZnO front contact was patterned by the UV or IR laser from film side, for the reference sample (Std.) IR laser patterning from the glass side is used. The active layers and back contact layers were patterned using our standard process.

4. Conclusions

In this article we used two Nd-doped solid state pulsed lasers to pattern ZnO thin-films from the film side. One IR laser with a wavelength of 1064nm and one UV laser with a wavelength of 355nm were used. For single pulses a smoother ablation of ZnO was obtained with the UV laser compared to the IR laser. Furthermore, using the UV laser we obtained craters with a lower rim and no sign of material melt. The ablation thresholds were determined with three different methods. The ablation threshold of ZnO for the IR is larger than for the UV. The differences in ablation thresholds are explained by the differences in absorption coefficients of the ZnO for the IR and UV. Both wavelengths can achieve good electrical separation even after deposition of a highly conductive µc-Si:H p-layer. In order to compare the various laser processes we prepared 10cm×10cm µc-Si:H modules on ZnO. We obtained comparable results for modules patterned from the film-side and modules patterned with the standard process.

Acknowledgements

The authors thank Joachim Kirchhoff and Hilde Siekmann for deposition of μc-Si:H p layers and ZnO, respectively, and Dr. Aad Gordijn for fruitful discussions.

References

[1] A. Buzas, Z. Geretovszky, Thin Solid Films. **515**, 8495 (2007).
[2] S. Haas, A. Gordijn, G. Schope, B.E. Pieters, H. Stiebig, SPIE, **6651**, H6510 (2007)
[3] O. Yavas, C. Ochiai, M. Takai. Appl. Phys. A, **69**, S875 (1999).
[4] A. D. Compaan, I. Matulionis, S. Nakade, Opt. Lasers Eng. **34**, 15 (2000).
[5] M. Berginski, J. Hüpkes, M. Schulte,G. Schöpe, H. Stiebig, B. Rech, M. Wuttig, J. Appl. Phys. **101**, 074903 (2007).
[6] J. M. Liu, Opt. Lett. **7**, 196 (1982).
[7] J. Bonse, J.M. Wrobel, J. Krüger, W. Kautek, Appl. Phys. A **72**, 89 (2001).
[8] B. Rech, T. Repmann, M. N. van den Donker, M. Berginski, T. Kilper, J. Hüpkes, S. Calnan, H. Stiebig, S. Wieder, Thin Solid Films **511–512**, 548 (2006).

*Corresponding author: s.ku@fz-juelich.de